Carcinogenicity of Fibrous Glass: Pleural Response in the Rat in Relation to Fiber Dimension[1]

[redacted]earl F. Stanton,[2] Maxwell Layard,[3] Andrew Tegeris,[4] Eliza Miller,[2] Margaret May,[2] *and* Elizabeth Kent[4, 5]

ABSTRACT—**Seventeen fibrous glasses of diverse type or dimensional distribution induced different incidences of malignant mesenchymal neoplasms when implanted in the pleurae of female Osborne-Mendel rats for periods of more than 1 year. Neoplastic response correlated well with the dimensional distribution of fibers. Fibers less than or equal to 1.5 μ in diameter and greater than 8 μ in length yielded the highest probability of pleural sarcomas, and probability trends suggested that pleural sarcoma incidence increased with increasing lengths of fibers with diameters of less than 1.5 μ. Morphologic observations indicated that fibers less than or equal to 8 μ in length were inactivated by phagocytosis. In fibers greater than 8 μ in length, the correlation of carcinogenicity with increasing length was difficult to explain. Since neoplastic response to a variety of types of durable fibers, particularly asbestos fibers, was similar, our experiments reinforce the idea that the carcinogenicity of fibers depends on dimension and durability rather than physicochemical properties and emphasize that all respirable fibers be viewed with caution.—J Natl Cancer Inst 58: 587-603, 1977.**

At the 1970 Symposium on Tissue Response to Asbestos held in Cardiff, Wales, we reported that exceptionally fine fibrous glass applied to the pleura of the rat induced sarcomas that were identical to the neoplasms induced with asbestos at this site and closely resembled mesotheliomas induced in the pleura of man by asbestos. Ancillary data suggested that the carcinogenicity of both asbestos and glass was related to the dimensional configuration of the fibers rather than to either their [redacted]ysicochemical properties or contaminating oils or [redacted]nerals. Further support for the concept that fiber carcinogenicity depended on durability and fibrous configuration of the proper dimension was attained in two subsequent reports in which the dimensional distribution of fibers of several types of asbestos, glass, and aluminum oxide was correlated with carcinogenicity (*1*, *2*). The present report extends these findings by more precise assessments of both carcinogenicity and the dimensional distribution of fibers in the 17 different types of fibrous glass tested thus far.

MATERIALS AND METHODS

Rats and implantation procedures.—The rats used and the method of exposing the pleura to fibrous glass were essentially those described in (*1*). We have consistently used female, specific-pathogen-free, Osborne-Mendel rats from the outbred, closed colony of the NIH Animal Production Section. As untreated controls, more than 4,000 old female Osborne-Mendel rats have been examined during the past 6 years. In our animal housing, the rats generally remained free of chronic pneumonitis, and no tumors were found in the thorax that might be confused with those induced in the pleura. At weaning, the litters were mixed randomly and the rats were housed 5 per large polycarbonate cage. They were fed commercially prepared rodent pellets and water ad libitum and treated between 12 and 20 weeks of age.

As in previous experiments, a substrate pledget of coarse fibrous glass was used as the vehicle for implanting the test fibers. In all experiments, the surface of flat, 45-mg pledgets composed of autoclaved, binder-coated, coarse fibrous glass of the type commonly used as insulation material, was coated with a standard dose of 40 mg test fibers that had been suspended in 1.5 ml of 10% gelatin by gentle continuous agitation. The gelatin-suspended coatings of test fiber were allowed to harden on the pledgets at 4° C, so that the pledgets developed a rubbery consistency. Treatment consisted of a left-sided open thoracotomy under ether anesthesia and the direct placement of the pledget over the visceral pleura. Application in this manner had several advantages: The pledgets could be manipulated easily so that the test fibers on the surface of the pledget could be applied uniformly to a broad surface of the visceral pleura. Additionally, it permitted the application of fibers that could not pass readily through a hypodermic needle, insuring that fibers were included that otherwise would have been fragmented or selectively filtered out by the injection procedures. Further, the coarse fibrous glass pledget acted as a partial barrier between the incision and the test material, thus retarding migration of the test fibers into the incision and surrounding tissues with the subsequent induction of tumors at extraneous sites.

Initially in each experiment, 30 rats were treated. The 1-3% of rats that died postoperatively within 3 weeks were replaced so that each group consisted of 30 long-term survivors. All groups were observed daily; only moribund rats were killed. An effort to insure long-term survival required the surgical removal of all mammary tumors as soon as they became palpable. The survivors were killed during the 25th month after treatment. Periodically during the progress of the experiments, groups of 30 rats were treated as controls with gelatin-saturated pledgets of the coarse fibrous glass vehicle, comparable in weight (85 mg) to the test fibers plus vehicle. The 130 treated control rats from these groups that died during the 24 months following treatment or that were randomly killed the 25th month after treatment comprised experiment #17 on which the calculations of significance are based. Gross necropsy findings were recorded on all rats, and histologic sections were examined after staining with H & E from all im-

ABBREVIATION USED: H & E = hematoxylin and eosin.

[1] Received July 6, 1976; accepted September 15, 1976.

[2] Laboratory of Pathology, National Cancer Institute (NCI), National Institutes of Health, Public Health Service, U.S. Department of Health, Education, and Welfare, Bethesda, Md. 20014.

[3] Biometry Branch, NCI.

[4] Pharmacopathics Research Laboratories, Inc., Laurel, Md. 20810.

[5] We are particularly indebted to the staff of the Johns-Manville Research and Engineering Center, Denver, Colo., and the Owens-Corning Fiberglas Corporation, Toledo, Ohio, for providing and characterizing many of the glasses studied.

ALL-STATE LEGAL® DEFENDANT'S EXHIBIT 16

HWBUI0006718

plant sites and all other grossly abnormal tissues. Special histologic stains were done occasionally.

Tested glass fibers.—The 17 tested fibrous glasses are listed in table 1 in order of decreasing carcinogenicity. They are designated by symbols that indicated their source, method of preparation, and relation to each other. The seven samples with a first letter designation "M" were processed by Dr. James Leineweber and the staff of the Johns-Manville Research and Engineering Center. Their methods of preparation, which consisted primarily of fragmentation of aqueous suspensions by blender and subsequent separation by centrifugation and filtration, have been published in (*3*). The M samples represent three starting batches of either flame-attenuated or rotary-processed borosilicate fibrous glass. The mineral content of the batches was similar to that of the fine fibrous glasses published in (*1*). Since milling was not used in sample preparation, the M samples were free of extraneous contamination and differed from each other only in dimension. The two M samples with a second letter designation "O" (used in expts 1 and 9) were from a single starting batch of fibers with nominal diameters below 1 μ. The third letter designation of these two samples indicated the aim of final separation into either long (L) or short (S) fibers. Similarly, the M samples with a second letter designation "6" (used in expts 3, 5, and 16) were from a starting batch of fibers of nominal diameter below 2 μ with the third letter designation indicating that the aim of final separation was to achieve either long (L), short (S), or whole (W) fibers (i.e., nonseparated fibers). Finally, the M samples with second letter designation "8" (used in expts 8 and 15) were from a batch of fibers of nominal diameter below 5 μ and again long (L) and short (S) lengths were the aim in separating the two samples.

The remaining four starting batches of fibrous glass were characterized in (*1*). The six samples with a first letter designation "K" (used in expts 2, 4, 6, 7, 10, and 12) were from a single batch of flame-attenuated borosilicate glass with a nominal diameter range of 0.06 to 3.0 μ and labeled AAA fibrous glass. Samples designated "KW" and "KL" (used in expts 2 and 4, respectively) represent the whole untreated K fibers and a modest attempt to shear these fibers to lengths that remained long but within a range that could be more easily measured. We did the shearing by processing an aqueous suspension of the whole fibers in a conventional Waring blender for three periods of 10 minutes and selecting sedimentation fractions that had predominating fibers greater than 50 μ in length. Samples designated "KCP," "KUP," "K2P," and "KFP" (used in expts 6, 7, 10, and 12) are the same K fibers processed primarily by comminution to short lengths in a Spex ball-mill with a stainless-steel ball and chamber. This treatment contributed significantly to contamination of the fibers by metallic deposition from the chamber. The duration of milling was 30 seconds for experiments 6 and 7, 2 minutes for experiment 10, and 10 minutes for experiment 12. Depending on the duration of milling, the additional content of the following metals was present in the samples by spectrographic analysis: chromium, 0.1-2.3%; copper, 0.001-0.025%; iron, 0.46-9.5%; magnesium, 0.01-0.02%; molybdenum, 0.002-0.015%; and nickel, 0.05-1.2%. In addition, sample KCP differed from the other K samples in that it retained a thin outer binder of heat-cured, urea-formaldehyde resin and small amounts of contaminating urea, mineral oil, and silicone.

Samples with first letter designations "O," "P," and "Y" were from three separate batches of fibrous glass of the type and size range commonly used commercially. These fibers had diameters three to five times greater than the M or K test fibers in the range of 5 and 25 μ—only rare fibers were less than 1 μ. All three samples had long fibers that required shortening for adequate application and measurement. Sample "O2P" (expt 11) was a silica-slag-derived mineral wool commonly used in the past as home insulation. It was composed of brittle, tapered fibers with hooklike attenuations that were highly irritating to the skin. This material contained higher levels of calcium and magnesium oxide than borosilicate glass and additionally was contaminated by metals from a 2-minute period of milling in a stainless-steel Spex mill. Sample "P2P" (expt 13) was a fibrous glass commonly used in filtration processes that contained higher levels of sodium and calcium oxides than conventional borosilicate glasses. It too was reduced to manageable lengths by comminution in the Spex ball-mill for 2 minutes with consequent contamination from this source. Finally, the two samples with the first letter designation "Y" (expts 14 and 17) were from typical, modern, insulation-type fibrous glass that was coated with a phenol-formaldehyde binder. This was the same coarse-diameter fibrous glass that served as the vehicle for implantation of all test samples in this series and in those reported previously. The fibers were twinning strands of exceptionally long length that necessitated approximations in the assessment of this dimension. Sample "YW" (expt 17), whole fibers from the pool employed as the vehicle, was simply increased in amount to equal the weight of the vehicle plus test sample. Sample "Y2P" was the same glass reduced to shorter fibers by comminution in the Spex ball-mill for 2 minutes. Like the other samples with third letter designations of "P," this sample also contained contaminating metal from the mill.

Estimation of particle size distribution.—Aliquots of each of the 17 samples were placed on microscopic slides and on Formvar-coated electron microscopic grids. When appropriate, these aliquots were diluted with distilled water and sonically vibrated to make more uniformly distributed suspensions. The preparations were then air dried. From each slide preparation, a series of microscopic fields thought to best represent the distribution of particles were photographed at final magnifications of ×100 to ×2,000 as appropriate to permit length and diameter measurements of each particle to the nearest 0.50 μ. In most cases, this required a series of step-wise magnifications of the same fields and the development of montages so that extremes in dimension could be adequately assessed. Approximately 1,000 consecutively counted particles within these fields yielded relatively stable ratios between a series of size ranges. At least

HWBUI0006719

1,000 particles were counted in each preparation except for those few with exceptionally long fibers. This tabulation of all particles visible by light microscopy insured a sufficient sample, but it did not adequately take into account particles less than 0.50 μ in diameter. Consequently, the grid suspensions were viewed in an AEI EM6B electron microscope and photographed at final magnifications of ×1,555 to ×19,698, and the diameter and length of each particle in the photographic fields were measured to the nearest 0.01 μ. Again, stepwise increases in magnification and montages were useful in measuring dimensional extremes. From 200 to 1,000 consecutively counted particles were measured; the number depended on the size distribution and the stabilization of ratios among the ranges of size studied. By light microscopic examination of the grids, particles of dimensions previously counted at light magnifications (generally particles with diameters >0.50 μ) could be separated from the submicroscopic particles, and a ratio between the optically visible particles and the submicroscopic particles could be determined. This ratio was used to calculate the number and dimensional distribution of submicroscopic particles presumed to be present in the fields of the 1,000 particles visible by light microscopy that had been counted previously. The dimensions of the total number of particles counted by light microscopy and those of the estimated total submicroscopic particles present in the same fields as those counted by light microscopy were then entered into an IBM 360-370 systems computer, and the following calculations were made for each sample.

Assuming the particles were cylindrical, we calculated the volume of each counted particle and converted this value to weight by multiplying by the density of glass. The weights of all counted particles were then summed to yield an estimate of the fraction of the standard 40-mg dose counted. From this estimate, either the number of particles of a given size in the standard 40-mg dose or the percent by weight occupied by particles of a given size could be calculated. The counted particles were then grouped into 34 dimensional ranges that seemed the most likely categories to show differences in response. These arbitrary ranges permitted simple illustrations of fiber distribution both by percent of the dose by weight that was occupied by each range or the number of particles per μg in each range (text-figs. 1, 2). Since it was probable that the count of numbers of particles was no more accurate than one order of magnitude, they were tabulated as the common log with the characteristic of the log representing the probable limit of accuracy.

RESULTS

Table 1 summarizes the results in terms of survival and tumor incidence. Whether or not pleural sarcomas developed, mortality was high especially during the second year after treatment. A scattering of tumors in other sites accounted for some deaths, but these neoplasms were not unusual in untreated controls and no significant trend in incidence could be related to treatment. In all groups, deaths from other than tumors resulted primarily from pneumonia, particularly when inflammation spread to the untreated right lung, since treatment partly compromised the total pulmonary reserve. For these reasons, the best estimate of neoplastic response depended on time of survival as well as the number of tumors.

Table 1 tabulates the time of death and whether or not a pleural sarcoma was present at death for each rat in the 17 experiments. From data similarly tabulated on a weekly basis, a standard actuarial life table method was used to estimate the overall probability of developing pleural sarcomas in each experiment (*4*, *5*). This computation, included in table 1, is derived in the following manner. Let n_x be the number of rats alive at the beginning of week x, and d_x be the number of rats dying of tumor in week x. Then the estimated probability that a rat which survives to the beginning of week x does not die with tumor in week x is

$$P_x = 1 - d_x/n_x.$$

The estimated probability that a rat dies with tumor by the end of week x is

$$q_x = 1 - P_1 \cdot P_2 \cdots P_x.$$

The method adjusts for rats that died early in the experiment without pleural sarcoma, which otherwise would cause the observed proportion of tumors to be less than the tumor probability, had all rats survived until they developed pleural sarcoma or the experiment was terminated. Since both treated control rats and the rats in the experimental groups were subjected to the same implantation procedure, the risk of dying from causes other than tumor was comparable for all groups. Therefore, the assumption underlying actuarial analyses appeared to be satisfied.

The estimated probabilities of pleural sarcoma in the 17 experiments ranged from 85.3% to zero. However, the results suggested division of the experiments into only three response groups excluding the treated controls (footnotes *c*, *d*, and *e* in table 1). The high-risk group consisted of experiments 1-5 from samples composed of either intact fibers or a fraction of the longest fibers from the glass samples with the finest diameters. The intermediate-risk group consisted of experiments 6, 7, and 8. Two of these three experiments were with fine fibers that had been reduced in length by milling, and the third consisted of the long-fibered fraction of large diameter (>2 μ). The eight experiments in the low-risk group (expts 9 through 16) were, for the most part, experiments with either large-diameter fibers or very short fibers.

In testing the combined experiments in each of the three groups for significant differences by the methods of Cox (*6*) and Mantel (*7*), we found that, in terms of tumor probability within groups, none of the individual experiments were significantly different from any other. However, the low-risk group was significantly different from the intermediate-risk group ($P<0.01$), which in turn was significantly different from the high-risk group ($P<0.0001$). The differences between the treated controls (expt 17) and the intermediate-risk and

HWBUI0006720

TABLE 1.—*Seventeen experiments with different types of fibrous glass ranked by probability of pleural sarcoma development*[a]

Sample designation	MOL	KL	M6L	KW	M6W	KCP	KUP	M8L	MOS	K2P	O2P	KFP	P2P	Y2P	M8S	M6S	YW
Experiment No. and rank	1	2	3	4	5	6	7	8	9	10	11	12	13	14	15	16	17
		High-risk group[c]				Intermediate-risk group[d]						Low-risk group[e]					
Probability of pleural sarcoma ±SD[b]	85.3 ±13.2	73.9 ±8.5	71.2 ±9.1	69.3 ±9.6	64.4 ±17.7	21.5 ±8.7	19.4 ±10.3	14.3 ±9.4	8.3 ±5.6	8.1 ±5.5	6.7 ±5.4	5.9 ±5.7	5.7 ±5.5	5.5 ±5.9	4.5 ±4.4	0	0
Wk after treatment	Number dying in stated period after treatment[f]																
6–52	0/13	0/1	0/1	0/5	0/8	0/2	0/4	0/2	0/3	0/2	0/5	0/3	0/5	0/6	0/1	0/2	0/15
53–56	0/1		1/0	1/1	0/1		0/2	0/1	0/1	0/1	0/1						0/3
57–60	2/0				0/3		0/2	0/1					0/5	0/2			0/17
61–64	1/0	1/0					0/1		0/1		0/5			0/1			0/12
65–68		0/1	1/0									0/2			0/1	0/1	0/6
69–72	1/0							0/1							0/1		0/4
73–76							1/0	0/3			0/2	0/1				0/2	0/2
77–80	1/0	1/0		1/0	1/2			0/2	0/1							0/1	0/2
81–84	1/5	1/0	1/0		1/0							0/1			0/1	0/1	0/1
85–88					1/1	1/1	0/2		1/0			0/1	0/1				0/2
89–92		0/1	1/1	1/0	1/1	1/0	0/1	0/2	1/1	1/0				1/0	0/3	0/1	0/4
93–96		3/0	2/3	0/1	1/2	1/0	0/2	1/4		0/2	0/1	0/2	0/1	0/1	0/1	0/3	0/12
97–100	0/1	3/0	2/0	2/0	1/2	0/4			0/1		0/1	0/2	1/1		1/0	0/4	0/9
101–104	3/1	11/7	10/7	11/7	1/3	2/18	2/13	1/12	0/20	1/23	1/14	1/17	0/16	0/19	0/21	0/15	0/41
Σ53–104	9/8	20/9	18/11	16/9	7/15	5/23	3/23	2/26	2/25	2/26	1/24	1/26	1/24	1/23	1/28	0/28	0/115

[a] All expts employed 30 long-term surviving rats except #17 (control, $n=130$). Standard doses of 40 mg test fibers used in all expts.
[b] Estimated actuarial probability of pleural sarcoma calculated on weekly death rate of rats surviving the first 52 wk after treatment.
[c] High-risk group: Probability of pleural sarcoma significantly higher than intermediate-risk group. Differences between expts within the group not significant.
[d] Intermediate-risk group: Probability of pleural sarcoma significantly higher than treated controls and low-risk group. Differences between expts within the group not significant.
[e] Low-risk group: Probability of pleural sarcoma significantly higher than untreated controls. Data insufficient to distinguish difference from treated controls. Differences between expts within the group not significant.
[f] Number with pleural sarcoma/No. without pleural sarcoma.

high-risk groups were both significant ($P<0.01$ and $P<0.0001$, respectively). However, the low-risk group was not significantly different from the treated controls at the 5% level ($P=0.1$) because the 130 treated controls were insufficient in number to exclude the possibility that single tumors might be the result of either the coarse glass fibers of the vehicle or simple nonspecific injury to the pleura. Subsequent to the completion of this study, three additional groups of treated controls were studied. Three pleural sarcomas were observed in a total of 150 rats from these groups. Thus, although the 1 or 2 neoplasms in the low-risk experiments were significantly different from untreated controls (*see* first paragraph in "Materials and Methods"), the specificity of low-level response seemed doubtful although it may have been the result of the large fibers of the vehicle.

The relationship of the high-, intermediate-, and low-response groups to particular types of fibers suggested, as in previous experiments (*1*, *2*), that tumor response was related to fiber dimension. A good indication of this relationship could be gained if one simply compared the high-, intermediate-, and low-risk probability groups as illustrated in figures 1–17. Ranked in order of tumor probability, the figures indicated that fineness of diameter and increasing length seemed related to carcinogenicity. To test this hypothesis, estimates of the distribution of particles by size were made in each experiment (as described in "Materials and Methods"), and these data were correlated with response. Text-figures 1 and 2 represent a series of dimensional grids, one grid for each experiment, with the fibers grouped into 34 categories of size and tabulated either as percentage of sample weight (text-fig. 1) or by the common logarithm of the number of particles per μg (text-fig. 2). The grid pattern was arranged so that, as one moved from lower left to upper right, the categories increased in diameter and length. Categories on the extreme left were essentially nonfibrous particles, and particles of the upper left categories frequently represented aggregates of submicroscopic particles and fibers. Categories on the right side of the grid were open-ended to accommodate the usual long fibers in many of the samples. In the submicroscopic ranges, fibers greater than 8 μ in length were often difficult to trace for their entire length and were included in the open-end categories. With ideal samples, particles in each sample should have been confined to a narrow range of adjacent categories. Obviously, this was not the case with most of the 17 samples, but the size distribution was sufficiently narrow in some samples to permit tentative conclusions. Comparison of the experiments at the two extremes of tumor probability (expt 1 vs. expts 16 and 17) indicated three patterns of nearly mutually exclusive fiber distribution. The high-risk experiment (expt 1) had a fiber distribution concentrated in the lower right categories of the grid, whereas the negative experiments (expts 16 and

HWBUI0006721

MOL-#1 85.3%	.01-1	1-4	4-8	8-64	>64
>8.0					
>4.0-8.0					
>2.5-4.0					
>1.5-2.5					
>.50-1.5		<1	<1	10	64
>.25-.50		<1		14	
>.10-.25		<1	<1	7	
>.05-.10			<1	3	
.01-.05			<1	1	

KL-#2 73.9%	.01-1	1-4	4-8	8-64	>64
>8.0					
>4.0-8.0					5
>2.5-4.0		<1	2	2	
>1.5-2.5	<1	1	3	38	
>.50-1.5	1	<1	19	28	
>.25-.50	<1	<1		<1	
>.10-.25	<1	<1	<1	<1	
>.05-.10	<1	<1	<1	<1	
.01-.05	<1	<1	<1	<1	

M6L-=3 71.2%	.01-1	1-4	4-8	8-64	>64
>8.0					
>4.0-8.0					
>2.5-4.0			2	3	
>1.5-2.5		<1	15	13	
>.50-1.5	<1	1	32	32	
>.25-.50	<1	<1	1		
>.10-.25	<1	<1	<1		
>.05-.10	<1	<1	<1		
.01-.05		<1	<1		

KW-#4 69.3%	.01-1	1-4	4-8	8-64	>64
>8.0			1	10	
>4.0-8.0			1	13	
>2.5-4.0			<1	11	
>1.5-2.5	<1	<1	1	30	
>.50-1.5	<1	<1	<1	30	
>.25-.50	<1	<1	<1		
>.10-.25			<1		
>.05-.10			<1		
.01-.05					

M6W-#5 64.4%	.01-1	1-4	4-8	8-64	>64
>8.0					
>4.0-8.0			2	<1	
>2.5-4.0	<1	<1	4	8	
>1.5-2.5	<1	1	10	11	
>.50-1.5	<1	1	2	27	30
>.25-.50	<1	<1	<1	2	
>.10-.25	<1	<1	<1	1	
>.05-.10	<1	<1	<1	<1	
.01-.05	<1	<1	<1	<1	

KCP-=6 21.5%	.01-1	1-4	4-8	8-64	>64
>8.0			11		
>4.0-8.0		3	18	43	
>2.5-4.0	<1	2	2		
>1.5-2.5	<1	1	5	1	
>.50-1.5	<1	3	2	3	4
>.25-.50	<1	<1	<1	<1	
>.10-.25	<1	<1	<1	<1	
>.05-.10	<1	<1			
.01-.05		<1	<1		

KUP-#7 19.4%	.01-1	1-4	4-8	8-64	>64
>8.0			<1	18	26
>4.0-8.0		1	4	11	3
>2.5-4.0		2	3	6	
>1.5-2.5	<1	6	6	7	5
>.50-1.5	<1	<1	<1	<1	
>.25-.50	<1	<1	<1	<1	
>.10-.25	<1	<1	<1	<1	
>.05-.10	<1		<1		
.01-.05					

M8L-#8 14.3%	.01-1	1-4	4-8	8-64	>64
>8.0					
>4.0-8.0					1
>2.5-4.0		<1	4	41	
>1.5-2.5	<1	<1	2	31	
>.50-1.5		1	<1	1	15
>.25-.50		<1	<1	<1	
>.10-.25				<1	
>.05-.10				<1	
.01-.05					

MOS-=9 8.3%	.01-1	1-4	4-8	8-64	>64
>8.0					
>4.0-8.0		11	45		
>2.5-4.0	6	12	2		
>1.5-2.5	9	1	<1		
>.50-1.5	2	5	1	1	
>.25-.50	1	1	1	1	
>.10-.25	<1	<1			
>.05-.10	<1	<1			
.01-.05	<1	<1			

K2P-#10 8.1%	.01-1	1-4	4-8	8-64	>64
>8.0					
>4.0-8.0					
>2.5-4.0	5	14	8		
>1.5-2.5	18	17	5		
>.50-1.5	3	23	6	1	
>.25-.50	<1	<1	<1		
>.10-.25	<1				
>.05-.10	<1	<1			
.01-.05					

O2P-#11 6.7%	.01-1	1-4	4-8	8-64	>64
>8.0				38	19
>4.0-8.0		9	18	<1	
>2.5-4.0	1	4	5	2	
>1.5-2.5	1	1	2	<1	
>.50-1.5	<1	<1	<1	<1	<1
>.25-.50	<1	<1	<1		
>.10-.25	<1	<1			
>.05-.10	<1				
.01-.05					

KFP-=12 5.9%	.01-1	1-4	4-8	8-64	>64
>8.0				49	
>4.0-8.0		18	10		
>2.5-4.0	6	8	<1		
>1.5-2.5	5	<1			
>.50-1.5	<1	2	<1	<1	
>.25-.50	<1	<1			
>.10-.25	<1				
>.05-.10	<1				
.01-.05					

P2P-#13 5.7%	.01-1	1-4	4-8	8-64	>64
>8.0				49	
>4.0-8.0		4	29	10	
>2.5-4.0	2	2	2		
>1.5-2.5	1	<1	<1		
>.50-1.5	<1	<1	<1	<1	
>.25-.50	<1				
>.10-.25	<1	<1			
>.05-.10	<1	<1			
.01-.05					

Y2P-#14 5.5%	.01-1	1-4	4-8	8-64	>64
>8.0				56	
>4.0-8.0		<1	30	4	
>2.5-4.0	1	2	5		
>1.5-2.5	1	<1	1		
>.50-1.5	<1	<1	<1	<1	
>.25-.50					
>.10-.25	<1	<1		<1	
>.05-.10					
.01-.05					

M8S-=15 4.5%	.01-1	1-4	4-8	8-64	>64
>8.0					
>4.0-8.0					13
>2.5-4.0	1	7	23		
>1.5-2.5	4	14	23		
>.50-1.5	1	6	6	3	
>.25-.50	<1	<1			
>.10-.25	<1				
>.05-.10	<1	<1	<1		
.01-.05					

M6S-=16 0%	.01-1	1-4	4-8	8-64	>64
>8.0					
>4.0-8.0					
>2.5-4.0					
>1.5-2.5	1		6		
>.50-1.5	5	34	26	18	
>.25-.50	2	4	1	<1	
>.10-.25	1	1	<1		
>.05-.10	<1	<1			
.01-.05	<1				

YW-#17 0%	.01-1	1-4	4-8	8-64	>64
>8.0				<1	83
>4.0-8.0				<1	14
>2.5-4.0				<1	3
>1.5-2.5				<1	<1
>.50-1.5				<1	<1
>.25-.50					
>.10-.25					
>.05-.10					
.01-.05					

Diameter μ

Length μ

TEXT-FIGURE 1.—Fiber distribution into 34 dimensional categories by percent of test sample weight for each of the 17 expts ranked by probability of pleural sarcoma.

HWBUI0006722

MOL-#1 85.3%

Diameter μ \ Length μ	>0.8	>4.0-8.0	>2.5-4.0	>1.5-2.5	>.50-1.5	>.25-.50	>.10-.25	>.05-.10	.01-.05
>0.8									
>4.0-8.0					2.23	2.53	3.23	3.08	
>2.5-4.0					3.08		3.95		
>1.5-2.5					2.93	3.35	4.53		
>.50-1.5						3.93	4.79		
>.25-.50						3.46	4.65		
>.10-.25									
>.05-.10									
.01-.05									

KL-#2 73.9%

Diameter μ \ Length μ				.01-1	>1-4	>4-8	>8-64	>64
			0.67					
		0.67	1.52	0.97				
	1.45	0.67	2.03	2.19				
	2.95	2.40	3.42	2.74				
2.55	3.16		3.63					
3.03	3.16	3.33	3.03					
2.85	4.09	3.76	3.25					
3.03	3.73	3.03	3.03					

M6L-#3 71.2%

Diameter μ \ Length μ	>0.8	>4.0-8.0	>2.5-4.0	>1.5-2.5	.01-1	>1-4	>4-8	>8-64	>64
			1.53	1.23					
		1.84	2.76	2.13					
>.50-1.5	2.81	2.05	2.59	3.70	2.90				
>.25-.50	2.44	2.44	3.16	3.39					
>.10-.25	2.44	3.52	3.44	3.62					
>.05-.10	2.44	3.44	3.56	3.70					
.01-.05		3.44	3.35	3.14					

KW-#4 69.3%

Diameter μ \ Length μ				.01-1	>1-4	>4-8	>8-64	>64
			0.06	0.06				
			0.36	0.76				
			0.06	1.06				
	0.66	0.37	1.41	1.98				
2.48	1.80	1.29	2.42	2.51				
1.06	0.67	1.70	2.75					
		1.67	2.71					
		1.67	2.51					
			2.21					

M6W-#5 64.4%

Diameter μ \ Length μ				.01-1	>1-4	>4-8	>8-64	>64
			1.10	1.58				
	1.10	1.09	1.95	1.10				
	1.10	2.18	2.74	2.01				
2.28	3.17	3.21	3.69	2.84				
1.40	2.84	3.11	3.54					
1.70	3.22	3.25	3.69					
3.10	3.55	3.47	3.76					
2.71	2.95	2.71	2.80					

KCP-#6 21.5%

Diameter μ \ Length μ	>8.0	>4.0-8.0	>2.5-4.0	>1.5-2.5	.01-1	>1-4	>4-8	>8-64	>64
	0.97								
	1.81	2.01	1.81						
	1.44	2.05	1.81						
	2.05	2.17	2.31	0.97					
>.50-1.5	3.00	3.59	3.17	2.85	2.01				
>.25-.50	3.24	3.38	3.10	2.55					
>.10-.25	3.24	3.28	3.10	2.50					
>.05-.10	2.50	2.90							
.01-.05	2.20	2.98	2.67						

KUP-#7 19.4%

Diameter μ \ Length μ				.01-1	>1-4	>4-8	>8-64	>64
		1.26	2.04	1.74				
	2.11	2.52	2.31	1.26				
	2.73	2.71	2.44					
2.88	3.93	3.54	3.19	1.96				
3.36	3.54	2.84	2.57					
3.36	3.50	2.61	2.31					
3.17	3.32	2.63	2.80					
	2.31		2.31					

M8L-#8 14.3%

Diameter μ \ Length μ				.01-1	>1-4	>4-8	>8-64	>64
			0.17					
		0.77	1.73	2.02				
	1.49	1.12	2.11	2.27				
	2.60	1.45	2.35	2.42				
	1.85		2.38					
			1.85					
			1.85					

MOS-#9 8.3%

Diameter μ \ Length μ	>8.0	>4.0-8.0	>2.5-4.0	>1.5-2.5	.01-1	>1-4	>4-8	>8-64	>64
		2.46	2.72						
	2.97	2.99	1.76						
	3.43	2.37	1.17						
>.50-1.5	3.88	3.91	2.76	2.46					
>.25-.50	4.34	4.02	3.69	3.37					
>.10-.25	4.43	3.88							
>.05-.10	5.90	4.19							
.01-.05	6.77	4.63							

K2P-#10 8.1%

Diameter μ \ Length μ				.01-1	>1-4	>4-8	>8-64	>64
	2.89	3.09	2.41					
	3.84	3.56	2.66					
4.12	4.53	3.60	1.81					
4.28	3.02	1.81						
4.11								
3.91	2.89							

O2P-#11 6.7%

Diameter μ \ Length μ				.01-1	>1-4	>4-8	>8-64	>64
			1.78	0.48				
		2.32	2.17	0.48				
	2.06	2.48	2.09	0.48				
	2.49	1.95	1.94	0.48				
2.83	2.83	1.91	1.84	0.48				
2.44	0.48	1.68						
2.08	1.65							
2.41								

KFP-#12 5.9%

Diameter μ \ Length μ	>8.0	>4.0-8.0	>2.5-4.0	>1.5-2.5	.01-1	>1-4	>4-8	>8-64	>64
	2.03								
	2.67	2.03							
	2.89	2.73	0.92						
	3.20	1.92							
>.50-1.5	3.19	3.48	1.52	0.92					
>.25-.50	2.96	1.22							
>.10-.25	3.30								
>.05-.10	3.27								
.01-.05									

P2P-#13 5.7%

Diameter μ \ Length μ				.01-1	>1-4	>4-8	>8-64	>64
			2.00					
		1.85	2.21	1.06				
	2.30	2.08	1.70					
	2.28	0.91	0.69					
2.56	2.51	1.21	0.81					
1.21								
2.36	1.29							
1.55	0.81							

Y2P-#14 5.5%

Diameter μ \ Length μ				.01-1	>1-4	>4-8	>8-64	>64
			1.96					
		1.08	2.24	0.60				
	1.94	2.12	2.16					
	2.58	1.74	1.64					
3.42	2.09	1.60	1.60					
3.12	1.60		1.30					

M8S-#15 4.5%

Diameter μ \ Length μ	>8.0	>4.0-8.0	>2.5-4.0	>1.5-2.5	.01-1	>1-4	>4-8	>8-64	>64
				1.37					
	2.21	2.75	2.90						
	3.17	3.43	3.29						
>.50-1.5	3.41	3.92	3.46	2.81					
>.25-.50	3.83	2.48							
>.10-.25	3.81								
>.05-.10	3.85	2.45	2.14						
.01-.05									

M6S-#16 0%

Diameter μ \ Length μ				.01-1	>1-4	>4-8	>8-64	>64
	2.45		2.85					
4.43	4.83	4.38	3.79					
5.17	4.88	3.87	2.15					
5.60	4.73	3.58						
5.45	4.28							
5.16								

YW-#17 0%

Diameter μ \ Length μ				.01-1	>1-4	>4-8	>8-64	>64
			0.89	0.34				
			0.92	0.40				
			0.80	0.30				
			T.00	0.11				
			T.10	0.41				

Diameter μ

Length μ

EXT-FIGURE 2.—Fiber distribution into 34 dimensional categories by common log of the number of particles per μg in each size category for each of the 17 expts ranked by probability of pleural sarcoma.

HWBUI0006723

17) had fiber concentrations in either the upper right or lower left categories of the grid. These three experiments suggested that fibers in the submicroscopic range (i.e., diameters, $\leq 0.5\ \mu$) and most likely those of greatest length in this range were the most carcinogenic. This impression was further augmented by the predominance of fibers with diameters of less than or equal to 0.25 μ and lengths of greater than 8 μ in the remaining four high-risk experiments. Furthermore, in the low-risk experiments (expts 9 through 16), the most consistent deficiencies in fiber distribution were in these same extremes of fineness and length. Two of the three experiments in the intermediate group (expts 6 and 8) also seemed to support the carcinogenicity of submicroscopic long fibers by yielding levels of this type of fiber that fell between those of the high-risk and low-risk groups. The failure of experiment # 7 to yield a higher probability of pleural sarcomas was the unexplained exception. Furthermore, the problem of a low, but potentially significant, risk of pleural sarcomas could not be limited to long fibers in the submicroscopic range, since these categories of fibers could not be detected in most of the experiments in the low-risk group.

Statistical regression techniques afforded a second more refined method of analysis. The logit transformation (*5*) was applied to the estimated tumor probabilities (P) according to the following formula:

$$\text{logit}=log\left(\frac{P}{1-P}\right).$$

To relate the logits to the particle size distribution, weighted linear regression methods were used. These methods find the linear function of the form

$$\text{logit}=a+B_1x_1+\cdots B_kx_k,$$

which best fits the data, where the x_i, $i=1, \cdots, k$, quantify certain features of the particle size distributions (e.g., common logarithm of the number of particles per μg or percent total weight in various size categories). The weights used in this analysis were the estimated standard errors of the tumor probability estimates, which were obtained from the life table analysis (table 1).

As previously noted, inspection of the data readily suggested that a concentration of particles in the relatively thin (diameter, $\leq 0.25\ \mu$) and long (length, $>8\ \mu$) dimensional categories was associated with higher probabilities of tumor. However, it was possible that there were other not easily observable relationships between tumor probability and the particle size distributions. This possibility was explored by the regression techniques described, using as explanatory variables either logarithms of numbers of particles or percent weight, in a variety of dimensional categories. No significant relationship between distributional factors and tumor probability was found, other than the evident positive correlation between "long and thin" particle concentration and tumor probability. A summary of correlation coefficients is given in table 2.

With the use of logarithms of numbers of fibers, two nonoverlapping size categories, used individually, were found to provide good fits to the data. The first of these included fibers with diameters less than or equal to 0.25 μ and lengths greater than 8 μ. The estimated regression equation was

$$log\left(\frac{P}{1-P}\right)=-3.06+0.993x,$$

with a correlation coefficient of 0.93, which reflects a highly significant relationship. The other category comprised fibers with diameters between 0.25 and 1.5 μ and lengths greater than 64 μ. The estimated regression equation was

$$log\left(\frac{P}{1-P}\right)=-3.14+1.340x,$$

with a correlation coefficient of 0.92, again reflecting a highly significant relationship. The graphs of these equations, together with the data points for each experiment, are given in text-figures 3 and 4. Since these two explanatory variables were so highly correlated with the logits of tumor probability, it was apparent that they must themselves be highly correlated, and indeed their correlation was 0.95. The consequence of this high correlation was that it was impossible to conclude, on the basis of these experiments, which group of fibers was the more important one for carcinogenesis.

Similar regression analyses with the use of percent of total weight of particles as explanatory variables led to diameters between 0.25 and 1.5 μ with lengths greater than 64 μ as the dimensional range which best explained tumor probability. The regression equation was

$$log\left(\frac{P}{1-P}\right)=-2.30+0.095x,$$

with a correlation coefficient of 0.88 (*see* table 2, text-fig. 5). For the range with a diameter of less than or equal to 0.25 μ and length of greater than 8 μ, the percent weight gave a relatively poor fit. The regression equation was

$$log\left(\frac{P}{1-P}\right)=-1.84+0.356x,$$

with a correlation coefficient of 0.51 (*see* table 2, text-fig. 6).

The equations described above could not be interpreted too rigidly because the estimated particle size distributions were subject to considerable sampling error, the range of dimensional variation in the glass types used was in some respects limited, and the particular choices of dimensional range as the explanatory variables were arbitrary and, to some extent, suggested by the data. Nevertheless, taken together, the regression analyses would suggest that glass fibers with diameters less than 1.5 μ and lengths greater than 8 μ were highly carcinogenic in the pleura of the rat and that fibers larger or smaller than these dimensions were less carcinogenic. Thus carcinogenic potential seemed determined by decreasing diameter until at or near the limits of optical visibility, but increasing length became an equally critical factor within this range.

Tissues at the site of implantation in rats dying during

HWBUI0006724

TABLE 2.—*Correlation coefficients of logit of tumor probability with [illegible] variables in different dimensional ranges of particle size*

Fiber length, μ	Fiber diameter, μ[a]			
	>4	>1.5–4	>0.25–1.5	0–0.25
0–8	−0.34	−0.45	0.00	0.11
	−0.29	−0.33	−0.41	−0.26
>8–64	−0.27	−0.09	0.65	0.93
	−0.40	−0.08	0.63	
>64	−0.10	0.63	0.92	0.51
	−0.27	0.42	0.88	

[a] *Upper figure* is correlation coefficient for number of particles/dose; *lower figure* is correlation coefficient for percent by weight of particles/dose.

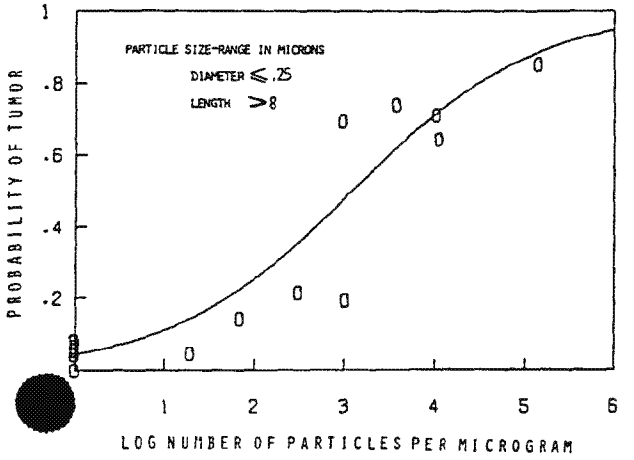

TEXT-FIGURE 3.—Regression curve relating probability of tumor to logarithm of number of particles per μg with a diameter of ≤0.25 μ and a length of >8 μ.

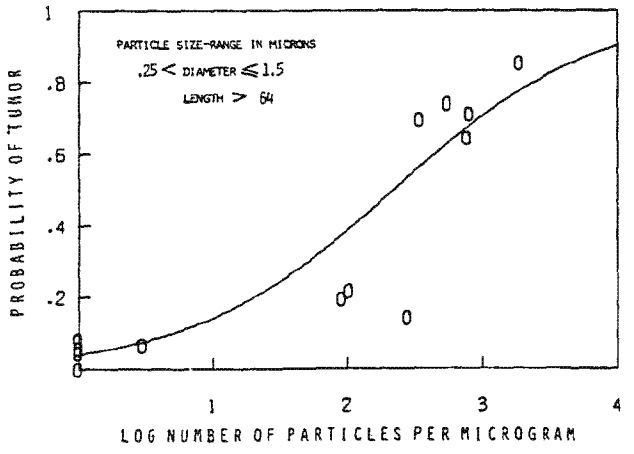

TEXT-FIGURE 4.—Regression curve relating probability of tumor to logarithm of number of particles per μg with 0.25 μ<diameter ≤1.5 μ and a length of >64 μ.

The experiments showed changes that could be assembled into a plausible series of events related to the development of the pleural sarcomas. The basic response to all [illegible] was typical of that to most foreign bodies, and in particular to the long, coarse fibers employed as vehicle and control. In the acute stage, hyperplasia of the mesothelium and vasodilatation, edema, and polymorphonuclear leukocyte infiltration of the adjacent connective tissue occurred. Tissue necrosis was minimal and the lung was only superficially affected. With all types of fibers, these acute changes at the pleural surface were promptly followed by mobilization and proliferation of vascular granulation tissue from mesenchyme which penetrated the overlying mesothelium and invaded the scaffold of glass fibers. Within the granulation tissue, polymorphonuclear leukocytes were replaced by mononuclear leukocytes, fibroblasts, and especially macrophages. The macrophages either engulfed small particles or adhered closely to large fibers, often fusing to form giant cells that effectively enclosed large fiber segments. For the most part, this process obscured the initially hyperplastic mesothelium, and a thick, uniform coat of vascular granulation tissue infiltrated the glass fibers and covered the affected lung surface. Slowly during the second year, the network of coarse, vehicle glass fibers collapsed and some fragments were carried away by macrophages. But vascular

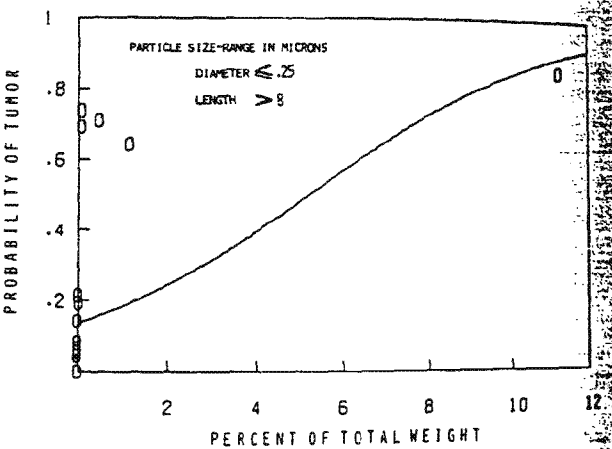

TEXT-FIGURE 5.—Regression curve relating probability of tumor to percent of total weight of particles with a diameter of ≤0.25 μ and length of >8 μ.

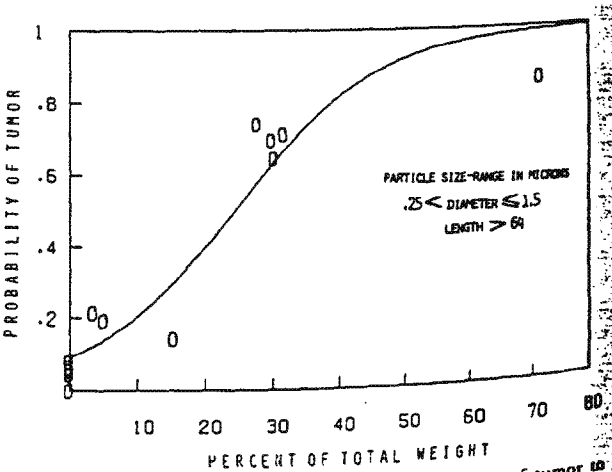

TEXT-FIGURE 6.—Regression curve relating probability of tumor to percent of total weight of particles with 0.25 μ<diameter ≤1.5 μ and a length of >64 μ.

granulatic
thelioid c
Notably,
The resp
cellular a
that migh
lesions ne
tion nor
signals th
Lesions
addition
essentiall
tosis see
stages, a
could be
With tim
short fib
sions at
scaffold
abundar
Again tl
even in t
of size.
On th
tained f
coarse
granula
viously
to accor
weeks,
the cell
Islands
part th
patchy,
abunda
with pl
in othe
ocytes
intrace
was no
The
sition
contai
wide c
these
experi
Altho
clear t
of ple
the e
site se
collag
Du
sarco
in str
pleur
oxide
those
cells,
morp
tics,

HWBUI0006725

[redacted]lation tissue permeated with macrophages, epithelioid cells, and foreign-body giant cells persisted. Notably, the lesions acquired a minimum of collagen. The response to these long, coarse fibers was highly cellular and often showed degrees of disorganization that might be confused with incipient neoplasia. But the lesions never extended beyond the site of fiber deposition nor did they show the anaplastic homogeneity that signals the onset of neoplasia (fig. 18).

Lesions that contained short fibers (expts 9-16), in addition to the long, coarse fibers of the vehicle, were essentially like those just described except that phagocytosis seemed far more successful. Even in the acute stages, an abundance of particle-laden macrophages could be found both at the site and in local lymph nodes. With time, it was apparent that only a small part of the short fibers was transported from the site. Pleural lesions at the end of 2 years had not only the collapsed scaffold of phagocyte-laden, coarse fibers, but also an abundance of short fibers entrapped within phagocytes. Again there was little evidence of collagen deposition even in the midst of abundant particles of both extremes of size.

On the other hand, lesions that predominantly contained fine, long fibers (expts 1-5), in addition to the coarse fibers of the vehicle, followed the pattern of granulation tissue proliferation and phagocytosis as previously described, but phagocytosis seemed inadequate to [redacted]ommodate the fine, long fibers. In as few as 8 [redacted] collagen had begun to accumulate and replace the cellular granulation tissue that invested the fibers. Islands of granulation tissue remained, but for the most part the reactive pleural covering was converted to a patchy, acellular, collagenous matrix which contained abundant, fine, long fibers seemingly free of contact with phagocytes or other inflammatory cells (fig. 19). As in other groups, regional lymph nodes contained phagocytes laden with the smaller fibers, but even though intracellular fibers were abundant, collagen deposition was not apparent in the nodes.

The link between fine, long fibers and collagen deposition was further supported by those experiments that contained small numbers of fine, long fibers among a wide distribution of fiber sizes (expts 6, 7, and 8). In these experiments, the extent of fibrosis was less than in experiments 1-5, but greater than in experiments 9-17. Although only rough comparisons could be made, it was clear that the degree of fibrosis matched the probability of pleural sarcomas. We had no conclusive indication of the exact site of tumor development, but a most likely site seemed to be mesenchyme trapped within the dense collagenous tissue.

During the course of the 17 experiments, 89 pleural sarcomas were observed. The tumors appeared similar in structure to those observed previously in rats with pleural implants of either glass, asbestos, or aluminum oxide fibers (*1*, *2*). The tumors could be divided into those composed almost entirely of elongated spindle ce[redacted]hose in which the cells assumed bizarre, polymo[redacted]ic configurations without identifiable characteristics, and those rare neoplasms that assumed an acinar or papillary epithelioid configuration (figs. 20-23). However, all three patterns seemed closely related, since they often merged in a single tumor, and no correlation between experiment and tumor pattern was apparent. The tumors frequently invaded mediastinal organs and occasionally implanted on the opposite pleura, but distant metastases were observed only rarely. One tumor was of particular note in that, although the primary tumor seemed composed entirely of spindle cells, implants of the tumor to the pleura of the opposite lung tended to show a papillary epithelioid differentiation (fig. 23).

DISCUSSION

The results of these experiments raise at least two points that merit discussion, the relationship of fiber dimension to mechanisms of carcinogenesis and the relevance of the findings to human exposure. An early paper (*1*) proposed that fibers at the lower range of optical visibility (i.e., diameters, $<1.5\ \mu$) that were exceptionally short (i.e., lengths, $<5\ \mu$) might account for the carcinogenicity of several types of glass and asbestos fibers. This hypothesis was not supported by subsequent data (*2*) which, along with those of the present report, indicate that the fine-diameter fibers that are long are carcinogenic and probably become more carcinogenic as their length increases. The negligible carcinogenicity of short fibers is perhaps related to the histologic observation that virtually all coarse- and fine-diameter fibers with lengths of $8\ \mu$ or less are efficiently entrapped by phagocytes. Many of the smallest particles are transported to regional lymph nodes, but even those that are not seem completely sequestered within the cytoplasmic limits of macrophages and foreign-body giant cells at the site of implantation. Similar observations have been made with chrysotile fibers in vitro (*8*). If we assume that efficient phagocytosis accounts for the lack of carcinogenicity of fibers less than or equal to $8\ \mu$ in length and that levels of tumor response depend on the quantity of fibers not effectively handled by phagocytes, we still must explain why fibers of coarse diameter that are long are less carcinogenic than fibers of fine diameter that are long. Considering that all rats were exposed to equal weights of the various types of fibers, obviously there were far more fine, long fibers than coarse, long fibers per dose. It also holds that fine fibers would have more ends and more surface area as well as a different surface curvature than comparable weights of long, coarse fibers. These differences suggest several hypotheses. It is reasonable that the ends of exceptionally fine fibers could penetrate both cell and nuclear membrane and cause varieties of damage that were not lethal. Nonlethal alteration of the genome is perhaps the simplest and most direct event that could initiate cancer. However, if cellular penetration is responsible for carcinogenesis, then the number of available fine fiber ends should determine the numbers of tumors. Consequently, equal weights of fine fibers of intermediate length should be more carcinogenic than fine fibers of long length. A careful review of the data suggests no

HWBUI0006726

evidence of this. Alternately, it has been proposed that the amount of fiber surface area available for cell anchorage might be critical to carcinogenesis (*9*), or that the tightly curved surface of fine fibers might alter anchorage sufficiently to cause cancer. Here again, if carcinogenicity depended simply on the amount of surface area of fine fibers, then equal weights of fine fibers of intermediate length should be equal in carcinogenicity to fine fibers of long length. Although there is some correlation between tumor incidence and the total surface area of fibers greater than 8 μ in length, the data are not sufficient to prove this hypothesis. In fact, a comparison of the intermediate-risk group with the high-risk group suggests that, without apparent difference in total surface area, exceptionally long length enhances carcinogenicity (*see* text-fig. 2, table 2). However, the process of phagocytosis, as it affects all sizes of fibers, needs to be taken into account if one intends to properly assess the number of free ends or the amount of free surface, and this is a problem that does not lend itself well to quantitation. Although present data are inadequate, there may be a direct correlation between tumor probability and the amount of fiber surface free of phagocytic activity. Further, since an apparent correlation exists between the amount of collagen in the lesion and the probability of pleural sarcoma, it is conceivable that collagen acts to block phagocytic activity on fiber surfaces. Collagen deposition alone is unlikely to induce cancer, but fine, long fibers entrapped within collagen and thus freed of phagocytic activity might play a key role.

Collagen deposition relates fiber carcinogenesis to the idea that pulmonary cancer in man is often associated with scarring (*10*) and to experimental carcinogenesis with inert solid sheets (*11, 12*). With solid sheets, carcinogenesis seems to depend on the development of a collagenous envelope at the site which is not unlike the pleural collagen induced by fine, long fibers. With both sheets and fibers, the collagen matrix may be uniquely dense and sufficiently ischemic to force the mutational selection of cells capable of uncontrolled proliferation (*13*). If collagen is a factor, then the question of its character and etiology arises. Our consideration of collagen or cancer mechanism is largely conjecture at the present time, but future experiments with fibers may be an advantage in the study of many questions concerning the general etiology of cancer.

It is of course not necessary to understand the mechanism to appreciate the relevance of these experiments to man. Many of the mesotheliomas of the pleura attributed to asbestos exposure in humans do not differ substantially from the sarcomas of the pleura induced in the rat with implants of the several types of asbestos that we and others have studied (*1, 14–16*). Even though inhaled asbestos reaches the human pleura by a different route than asbestos implanted in the experimental animal, it is unlikely that proximal mechanisms of asbestos carcinogenesis differ in rodents and man. It is our contention that the proximal carcinogenicity of asbestos depends primarily on its exceptionally fine, long dimensions and durability rather than on physicochemical properties (*2*). It follows then that durable fibers of other types should be equally carcinogenic and yield the same types of tumors if they attain the exceptionally fine, long dimensions of asbestos. In the rat, this would seem to be true of the variety of fibers that we have studied thus far, including the glass fibers reported here. To date we have induced significant numbers of pleural sarcomas in rats with fine, durable fibers of the following types: chrysotile, crocidolite, amosite, tremolite, glass, attapulgite, dawsonite, aluminum oxide, silicon carbide, and potassium titanate. Appropriate nonfibrous controls suggest that foreign materials other than long, fine fibers may cause fibrosis, but they do not induce significant incidences of pleural sarcomas. It seems reasonable then to assume that all dusts that contain fine, long, durable fibers represent a potential hazard to man. Certainly, any measurements of human exposure or consideration of tolerance levels for human exposure should take into account not only the variety of the fiber but also the dimensional character of the fiber.

We have emphasized previously that our experiments explore mechanisms of fiber carcinogenesis at the proximal site of susceptible tissues rather than acting as an estimate of the overall hazard of different fibers to man (*1*). Clearly, fibers must have the opportunity to reach the target tissue to cause cancer. Our experiments are inappropriate for evaluating many aspects of the environmental hazard, since they circumvent those factors that might inhibit or enhance exposure through natural routes. Subtle structural differences in different types of fibers may influence the aerodynamic properties of fibers as well as their penetrability and clearance from the lung. These factors would seem to play an important role in pulmonary exposure to different types of asbestos (*17–19*), and similar factors may well apply to other types of fibers. Although several well-executed inhalation studies with glass particles in animals have indicated no adverse effects (*20–22*), we believe these experiments have not entirely resolved the issue of carcinogenesis by inhalation, since the experiments were in part handicapped by insufficient quantitative measurements of fiber size and dose. Inhalation experiments with glass fibers in narrowly limited dimensional ranges, particularly those ranges found to be the most carcinogenic in the present study, should offer a broad base from which guidelines of safety might be determined.

In the past, it has often seemed that only the painful truth of epidemiologic evidence was sufficient to arouse concern for a potential environmental hazard. It is reassuring then to learn that at present it is unlikely that anyone has been exposed to quantities of airborne glass fibers of a variety and size comparable to levels of asbestos fibers that are considered to be even minimally hazardous to man (*23–32*). These references also suggest that fibrous glass of the conventional type and dimension has not been a demonstrable cancer hazard to either man or experimental animal, presumably because it exceeds the dimensional range that is carcinogenic. However, unequivocal evidence regarding the response of man to inhaled particles of glass would require the study of far more individuals for much longer times and

HWBUI0006727

[redacted] exposed to higher levels than those currently re[redacted]. Our experiments indicate that the hazard may largely be confined to long fibers of exceptionally fine diameter. Glass fibers of this type have a limited commercial usage and the hazard of exposure seems remote from the more likely exposure to asbestos. Nevertheless, it would seem prudent to regard all respirable fibers with caution. Hopefully, well-designed inhalation experiments will establish safety guidelines, and reasonable monitors and safeguards will make epidemiologic data an impossible achievement.

REFERENCES

(1) STANTON MF, WRENCH C: Mechanisms of mesothelioma induction with asbestos and fibrous glass. J Natl Cancer Inst 48:797–821, 1972

(2) STANTON MF: Some etiological considerations of fibre carcinogenesis. *In* Biological Effects of Asbestos (Bogovski P, Timbrell V, Gilson J, et al, eds.). Lyon, France, World Health Organization, International Agency for Research on Cancer, Publication No. 8, 1973, pp 289–294

(3) SPEIL S, LEINEWEBER J: Personal experiences with making samples of fibres for biological experiments. *In* Fibres for Biological Experiments (Pelnar PV, ed). Montreal, Canada, Institute of Occupational and Environmental Health, 1974, pp 45–50

(4) PILGRIM HI, DOWD JE: Correcting for extraneous death in the evolution of morbidity or mortality from tumors. Cancer Res 23:45–48, 1963

(5) ARMITAGE P: Statistical Methods in Medical Research. New York, John Wiley & Sons, 1971, pp 376–377, 410–414

(6) COX D: Regression models and life tables. J R Stat Soc [B] 34:187–220, 1972

(7) MANTEL N: Chi-square tests with one degree of freedom; extensions of the Mantel-Haenszel procedure. J Am Stat Assoc [redacted]:690–700, 1963

([redacted]) [redacted]ISON A: Experimental methods—cell and tissue culture: Effects of asbestos particles on macrophages, mesothelial cells and fibroblasts. *In* Biological Effects of Asbestos (Bogovski P, Timbrell V, Gilson J, et al, eds.). Lyon, France, World Health Organization, International Agency for Research on Cancer, Publication No. 8, 1973, pp 89–93

(9) MAROUDAS N, O'NEAL C, STANTON M: Fibroblast anchorage in carcinogenesis by fibres. Lancet 1:807–809, 1973

(10) RAEBURN C, SPENCER H: Lung scar cancers. Br J Tuberc 51:237–245, 1957

(11) OPPENHEIMER B, OPPENHEIMER E, STOUT A, et al: The latent period in carcinogenesis by plastics in rats and its relation to the presarcomatous stage. Cancer 11:204–213, 1958

(12) BRAND K, BUOEN L, JOHNSON K, et al: Etiological factors, stages, and the role of the foreign body in foreign body tumorigenesis: A review. Cancer Res 35:279–286, 1975

(13) ALEXANDER P, HORNING E: Observations on the Oppenheimer method of inducing tumors by subcutaneous implantation of plastic films. *In* Carcinogenesis: Mechanisms of Action (Wolstenholme G, O'Connor M, eds.). Boston, Little Brown & Co., 1959, pp 12–25

(14) WAGNER JC: The pathogenesis of tumors following the intrapleural injection of asbestos and silica. *In* Morphology of Experimental Respiratory Carcinogenesis (Nettesheim P, Hanna MG, Deatherage JW, eds.). Oak Ridge National Laboratory, Oak Ridge, Tennessee, Atomic Energy Commission Symposium Series No. 21, 1970, pp 347–358

(15) MAGNER D, MCDONALD AD: Malignant mesothelial tumors. Histologic type and asbestos exposure. N Engl J Med 287:570–571, 1972

(16) CHURG J, ROSEN SH, MOOLTEN S: Histological characteristics of mesothelioma associated with asbestos. Ann NY Acad Sci 132:614–622, 1965

(17) TIMBRELL V, GRIFFITHS DM, POOLEY FD: Possible biological importance of fibre diameters of South African amphiboles. Nature 232:55–56, 1971

(18) TIMBRELL V: Physical factors as etiological mechanisms. *In* Biological Effects of Asbestos (Bogovski P, Timbrell V, Gilson JC, et al, eds.). Lyon, France, World Health Organization, International Agency for Research on Cancer, Publication No. 8, 1973, pp 295–303

(19) GILSON JC: Asbestos cancer: Past and future hazards. Proc R Soc Med 66:395–403, 1973

(20) SCHEPERS G: Pulmonary histologic reactions to inhaled fiberglas-plastic dust. Am J Pathol 35:1169–1187, 1959

(21) GROSS P: The effects of fibrous glass dust on the lungs of animals. *In* Symposium on Occupational Exposure to Fibrous Glass, vol 2. Rockville, Maryland, National Institute for Occupational Safety and Health, 1974, pp 31–38

(22) KUSHNER M: The effects of intratracheal instillation of glass fibers of varying size in guinea pigs. *In* Symposium on Occupational Exposure to Fibrous Glass, vol 2. Rockville, Maryland, National Institute for Occupational Safety and Health, 1974, pp 20–31; quoted by Gross P: The biological categorization of inhaled fiberglass dust. Arch Environ Health 31:101–107, 1975

(23) National Emission Standards for Hazardous Air Pollutants: Federal Register 40(199):48292–48311, 1975

(24) ENTERLINE PE, DECOUFLE P, HENDERSON V: Respiratory cancer in relation to occupational exposures among retired asbestos workers. Br J Indust Med 30:162–166, 1973

(25) British Occupational Hygiene Society Committee on Hygiene Standards: Hygiene standards for airborne amounts of asbestos dust. Ann Occup Hyg 16:1–5, 1973

(26) BJURE J, SODERHOLM B, WIDIMSKY J: Cardiopulmonary function studies in workers dealing with asbestos and glasswool. Thorax 19:22–29, 1964

(27) NEWHOUSE ML: Asbestos in the work place and the community. Ann Occup Hyg 16:97–102, 1973

(28) HILL JW, WHITEHEAD WS, CAMERON JD, et al: Glass fibres: Absence of pulmonary hazard in production workers. Br J Indust Med 30:174–179, 1973

(29) ENTERLINE P, HENDERSON V: The health of retired fibrous glass workers. Arch Environ Health 30:113–116, 1975

(30) CORN M, SAVSONE E: Determination of total suspended particulate matter and airborne fiber concentrations at three fibrous glass manufacturing facilities. Environ Res 8:37–52, 1974

(31) GROSS P, TUMA J, DETREVILLE R: Lungs of workers exposed to fiberglass. Arch Environ Health 23:67–76, 1971

(32) SHULTE P, ed: Occupational exposure to fibrous glass. *In* Proceedings of a Symposium of the National Institute for Occupational Safety and Health. DHEW Publication No. (NIOSH 76-151). Washington, D.C., U.S. Govt Print Off, 1976

HWBUI0006728

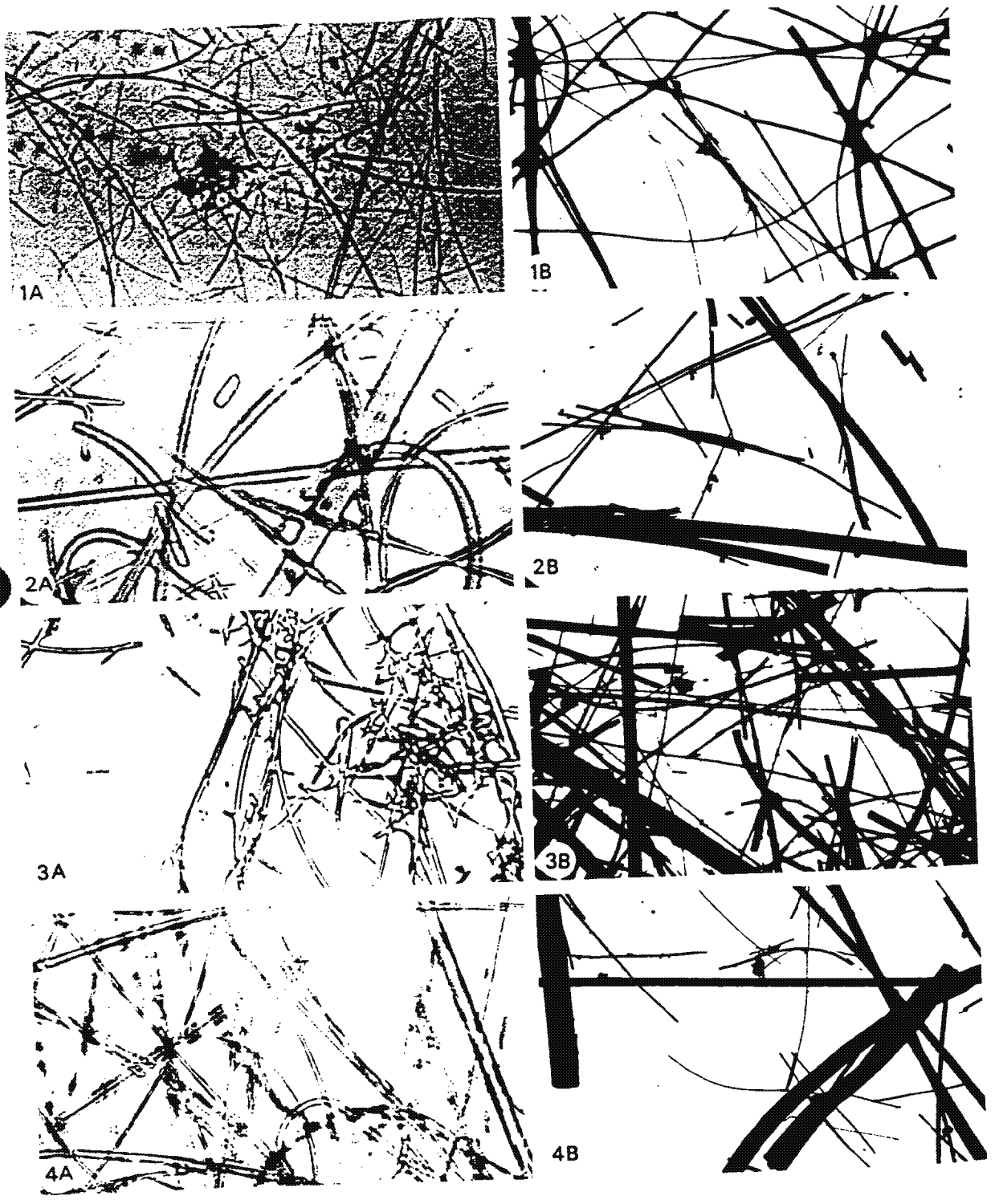

FIGURES 1-17.—Silhouettes of samples of the 17 types of glass fibers used. Figures are numbered to correspond to the experiment number and rank for probability of inducing pleural sarcoma. Figures A are all at × 750; figures B are all at × 3,200.

HWBUI0006729

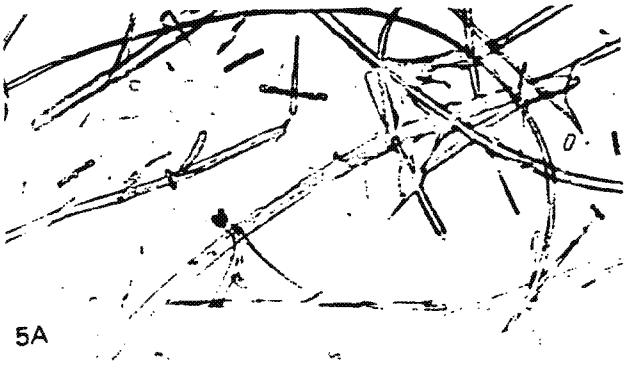

5A



5B



6A



6B

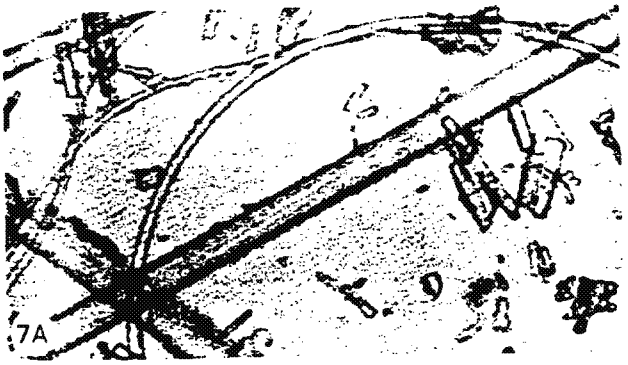

7A



7B

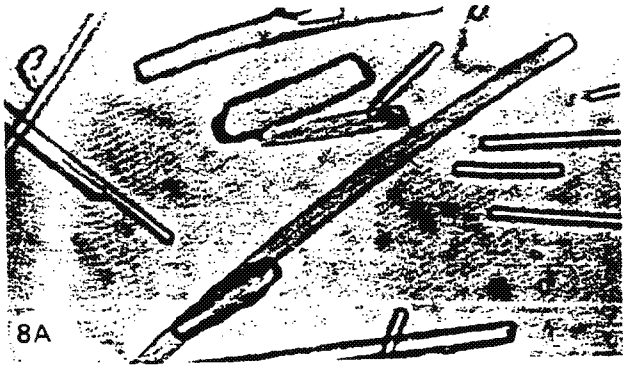

8A

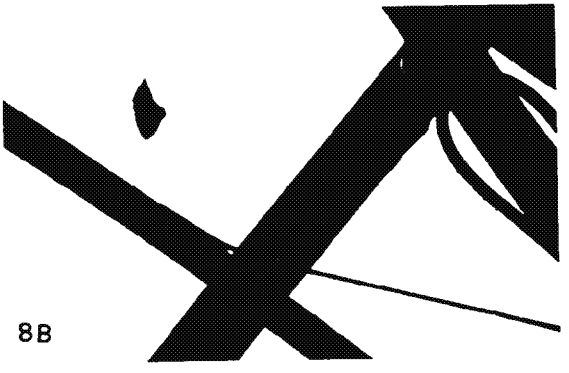

8B

HWBUI0006730

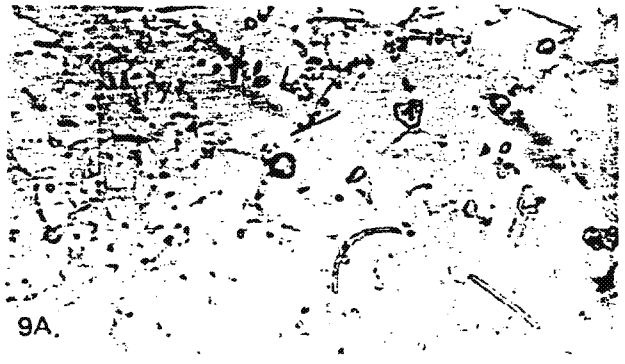

9A.

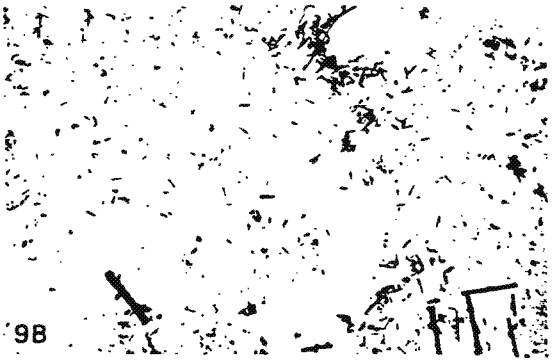

9B



10A

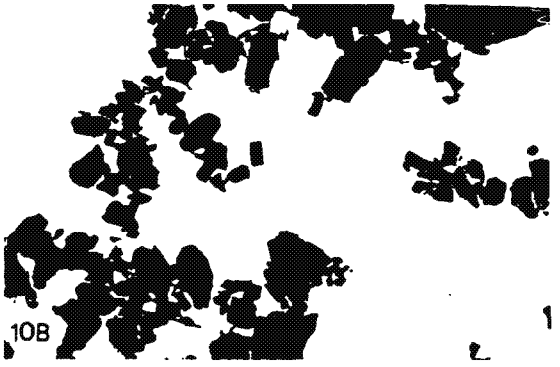

10B

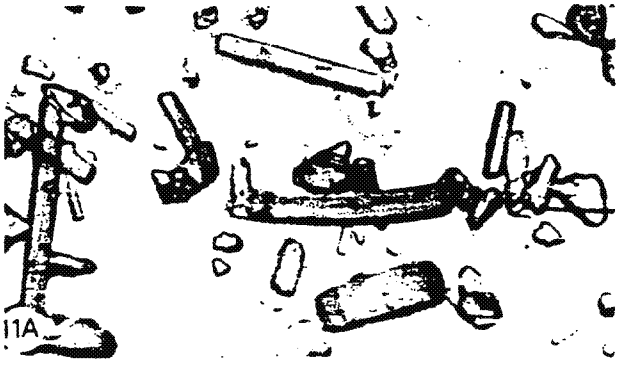

11A



11B

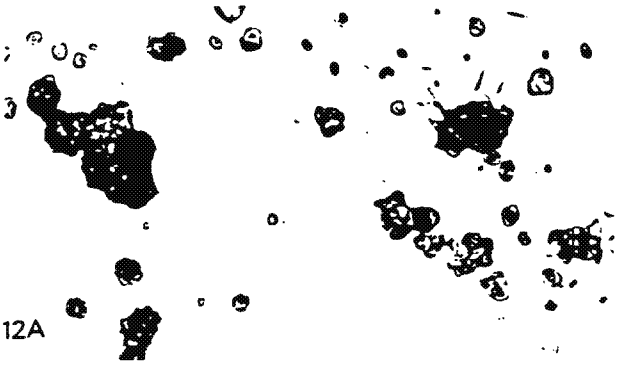

12A



12B

HWBUI0006731

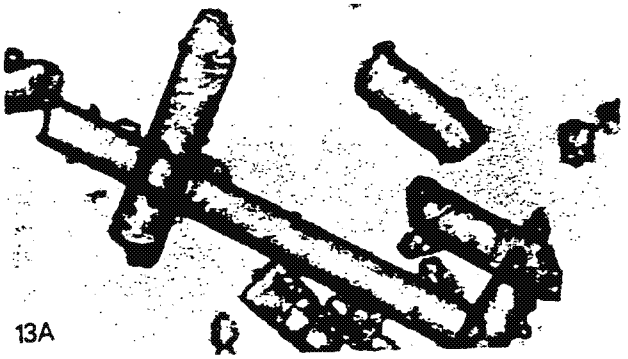

13A



13B



14A



14B



15A

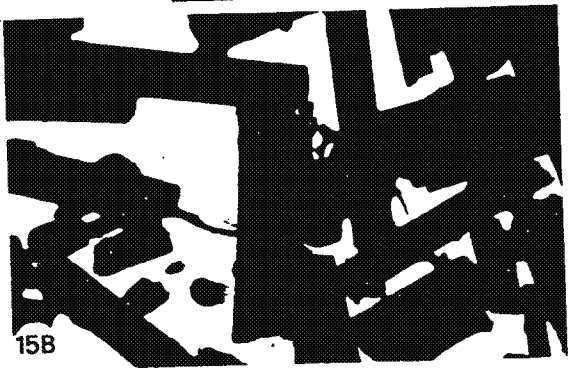

15B

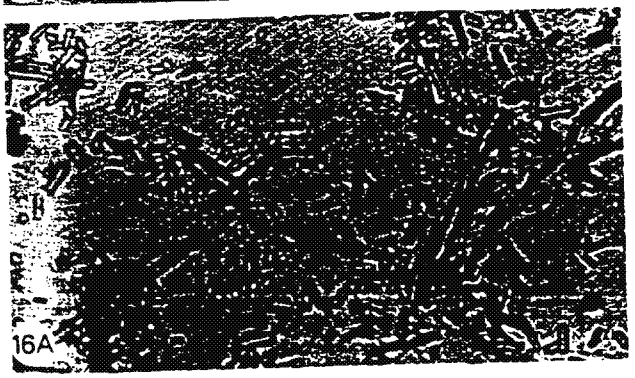

16A



17B

HWBUI0006732

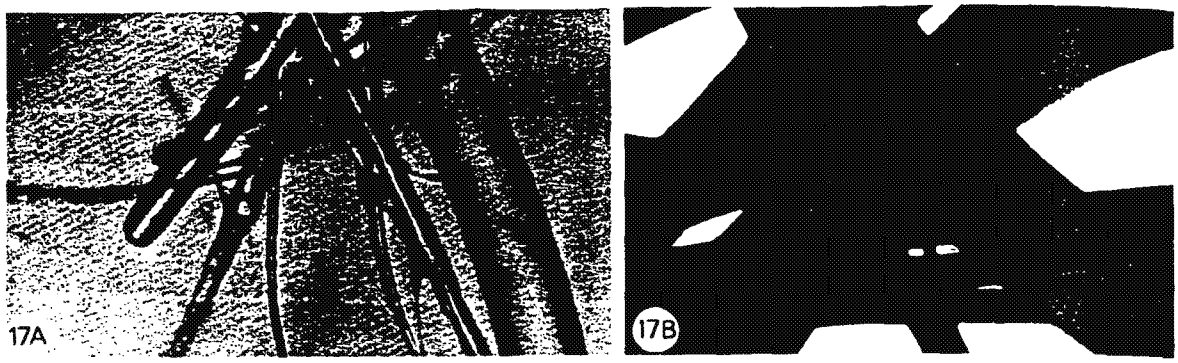

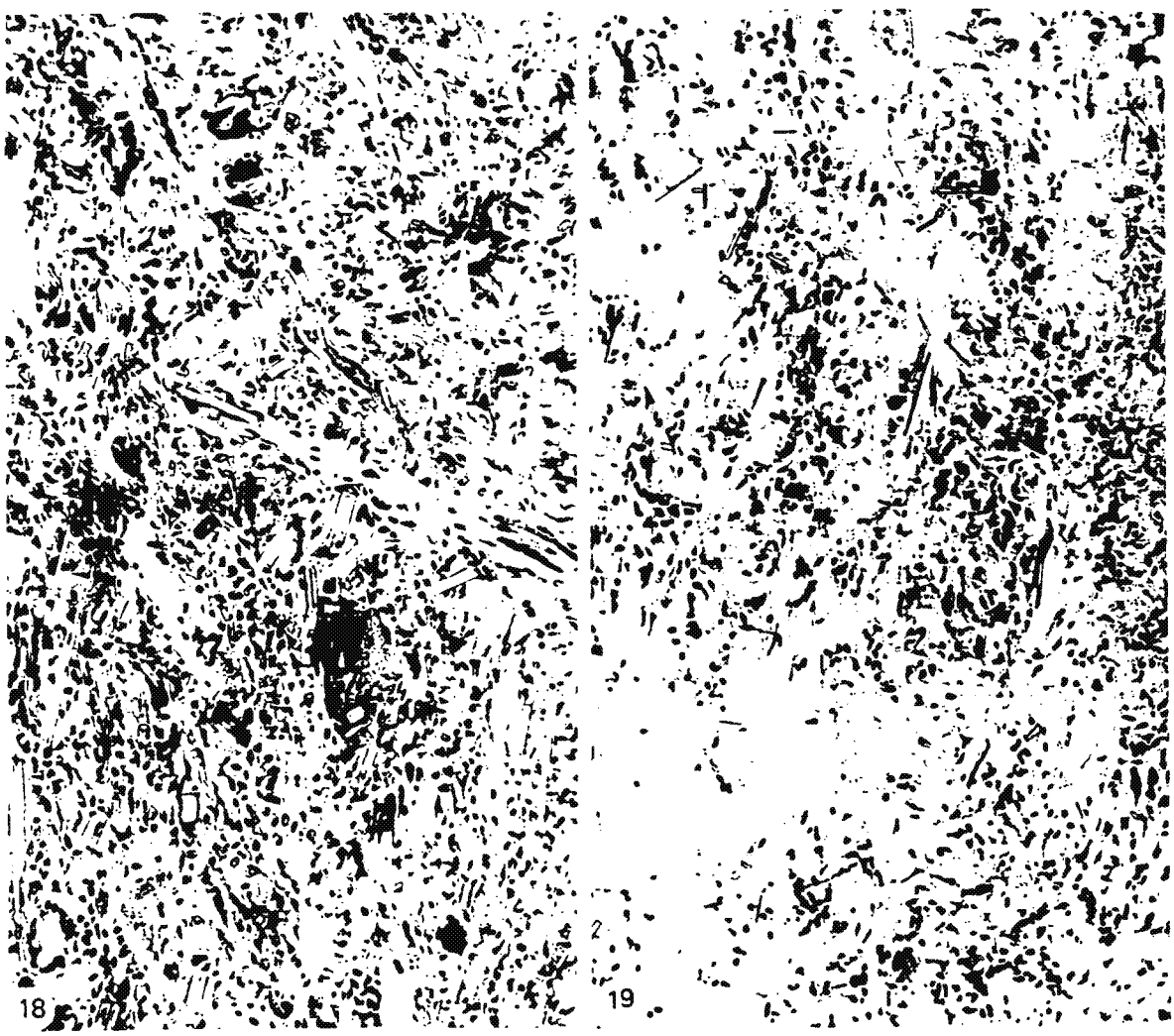

FIGURE 18.—Typical pleural response to noncarcinogenic glass fibers. *Note* phagocytic activity around large-diameter vehicle glass and minute particles of glass, from expt M6S-#16. H & E. × 100

FIGURE 19.—Typical preneoplastic pleural response to carcinogenic glass fibers. *Note* numerous fine, long fibers in dense acellular matrix and patchy character of the granulomatous response, from expt KL-#2. H & E. × 100

HWBUI0006733

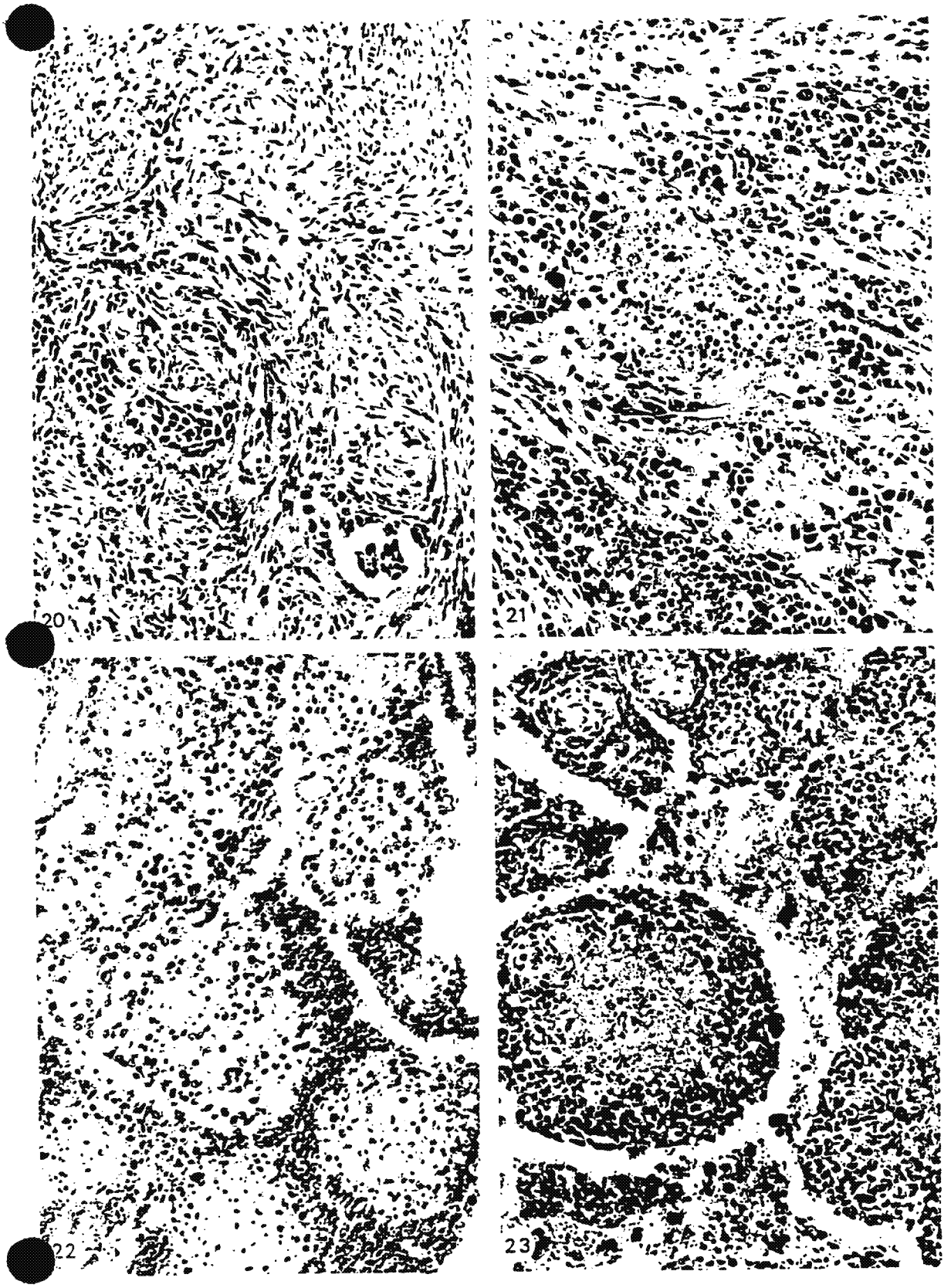

FIGURES 20–23.—Pleural sarcomas with characteristics that range from spindle to pleomorphic to tubulopapillary epitheloid cell patterns. *See* also (*1*) and (*2*). Figure 23 is a papillary pleural implant from pleural sarcoma of contralateral pleura composed predominently of spindle cells. H & E. × 100

HWBUI0006734